Towards Rocket Plume Assisted In-Situ Construction Processes Supporting Extraterrestrial Exploration Activities

Addison Holcomb[1] and Katsumasa Kawahara[2]

Louisiana State University, Baton Rouge, Louisiana, 70808, United States of America

I. Abstract

Sustained human activity on the Moon and Mars will require in-situ resource utilization (ISRU) and the ability to construct load-bearing landing and launch pads directly from local regolith. This work investigates the first stage of a proposed plume-assisted construction method in which solid, resin-filled pellets are entrained into a rocket exhaust plume and embedded into lunar or Martian soil. Subsequent heating would release and cure the resin, forming a bonded foundation. The present study focuses on demonstrating pellet entrainment and embedding using a bench-scale cold-flow apparatus and complementary computational modeling. The experimental setup consists of a vertically oriented cylinder supplying compressed air to a 3-D printed converging–diverging nozzle with an injection port downstream of the throat. Reflective glass pellets with 1 mm diameter are introduced through a secondary chamber, and inlet temperature is controlled using an external heater. Pressure and temperature sensors characterize inlet conditions. A CFD model developed in ANSYS Fluent provides insight into the internal nozzle flow and expected exit conditions under supersonic regimes that are difficult to measure experimentally. Initial attempts to match lunar landing Reynolds and Mach numbers were limited by laboratory pressure constraints; isentropic analysis showed that achieving the required Reynolds number would demand stagnation temperatures near 3500 °C. The study therefore shifted toward matching lunar-relevant exit velocities of approximately 950 m/s. Preliminary experiments confirm successful pellet injection into the cold-flow plume. Planned testing will increase inlet temperature to 627 °C to achieve the target exit velocity and will incorporate Particle Image Velocimetry and infrared imaging to measure particle velocity and temperature. Embedding performance will be evaluated using clay or sand substrates. Early 2-D CFD results predict an exit velocity of 925 m/s for a nozzle area ratio of 1.92. The final paper will present combined experimental and computational findings, including particle transport behavior and the feasibility of plume-assisted regolith binding for extraterrestrial landing pad construction.

II. Nomenclature

P_0	=	stagnation pressure
T_0	=	stagnation temperature
P_s	=	static pressure
T_s	=	static temperature
A_e	=	nozzle exit area
$A*$	=	nozzle throat area
$A_e/A*$	=	nozzle expansion ratio
M_e	=	exit mach number
v	=	particle velocity
Δx	=	change in position
Δt	=	change in time

[1] Undergraduate Student, LSU Mechanical Engineering, and AIAA University Student Member (1923595)
[2] Undergraduate Student, LSU Mechanical Engineering, and AIAA University Student Member (1921662)

v_0 = initial velocity
k = constant
n = number of frames

III. Introduction

The success of extraterrestrial exploration depends on the ability to deliver humans, robots, and cargo to specific landing sites without the constraints of natural landscape geology. Sustained presence on the Moon and Mars necessitates in-situ resource utilization (ISRU) to mitigate the prohibitive costs of transporting construction materials from Earth. A primary challenge in this domain is plume-surface interaction (PSI), which occurs when rocket exhaust impinges upon loosely consolidated regolith. This interaction results in surface erosion, granular flow, and the high-velocity ejection of dust and debris, which can damage landing hardware and existing planetary assets. In 1969, the Apollo 12 lunar module landed approximately 160 meters away from the Surveyor III probe. Ejecta from the landing sandblasted the lunar asset with lunar dust traveling at speeds up to 3,000 m/s damaging equipment.

To address these challenges, this research serves as a proof of concept for the in-situ construction of resilient, load-bearing landing and launch pads. The methodology is based on the Masten In-Flight Alumina Spray Technique (FAST), which seeks to mitigate plume-surface interaction (PSI) effects by creating a load bearing landing pad under a vehicle as it descends. This technology utilizes the rocket exhaust plume as both a momentum source and a thermal energy source. In this sequence of operations, solid pellets containing high-temperature-resistant polymer resin are injected into the supersonic exhaust stream and embedded into the Lunar or Martian regolith. Subsequent heating from the plume facilitates the release of the resin, leading to curing, cross-linking, and the synthesis of a polymer-regolith composite.

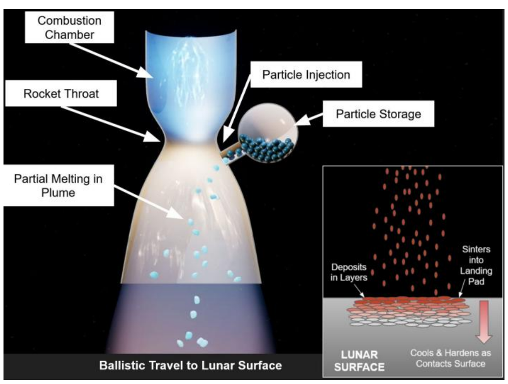

Figure 1: Concept of Particle Injection Within Plume

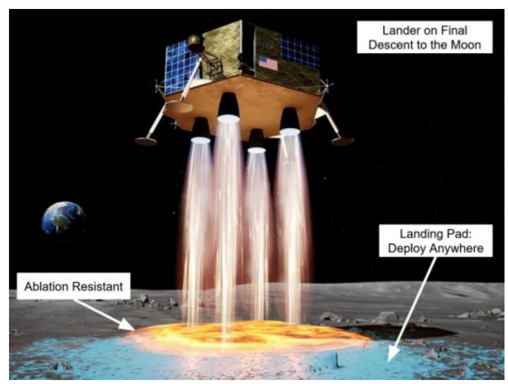

Figure 2: Rendering of Masten's FAST

Whereas prior studies have focused primarily on the modeling of under-expanded gas jets and resulting erosion physics, this work investigates the discrete-phase mechanics of particle entrainment and thermal coupling within the plume. The investigation utilizes a multi-disciplinary approach, combining experimental diagnostics with computational fluid dynamics (CFD). High-speed two-phase flow research is conducted using particle image velocimetry (PIV) and infrared (IR) imaging to characterize particle velocity and temperature. Furthermore, the mechanical integrity of the resulting foundations is evaluated using compositionally and geotechnically analogous simulants. This data is essential for establishing a baseline for the construction of sustainable spacecraft platforms, ultimately aligning with strategic goals for long-term extraterrestrial utilization.

IV. Experiment

A. Experimental Approach

The original apparatus for this experiment was utilized and developed by a previous graduate student. Modifications and additions were made to the previous apparatus to conduct the following experiment. Compressed air is supplied by an outdoor compressor to a 9.7 m^3 accumulation tank maintained at 689.5 kPa (100 psi) for the experiment. From the tank, the air passes through a dryer and a pressure regulator to establish the specific stagnation conditions required for each test case. As shown in the schematic in Fig. X, the air is routed from a 25.4 mm (1") primary line into the apparatus via 9.5 mm (3/8") nylon tubing. Connected to the flexible tubing is a rigid pipe which is attached to the cylinder through a 9.5 mm (3/8") Schedule 40 pipe cross, which serves as a junction for instrumentation ports. The data from the instrumentation is acquired via an NI cDAQ data acquisition system and recorded using a LabVIEW program.

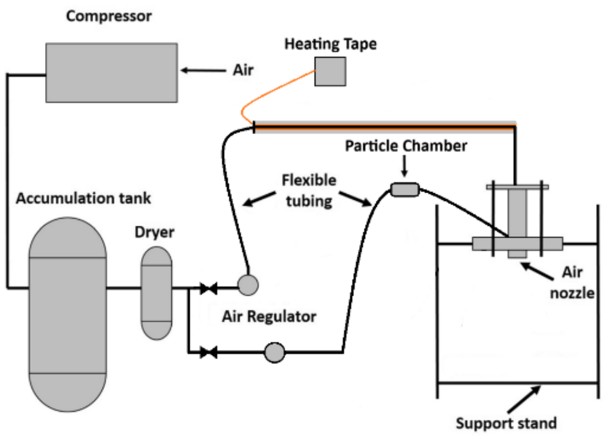

Figure 3: Schematic of Experiment

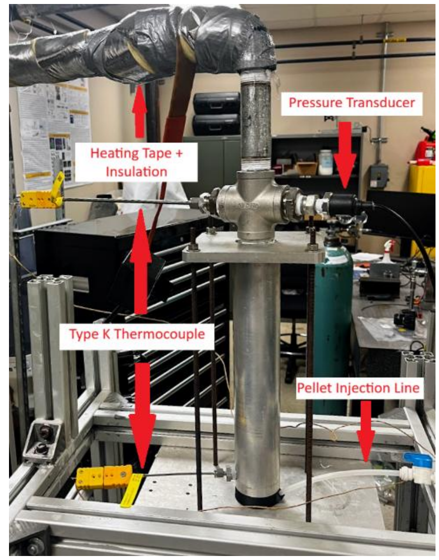

Figure 4: Image of Apparatus

To simulate the high-energy environment of a rocket plume, the rigid piping connected to the vertical test cylinder is externally wrapped with BriskHeat 120V silicone rubber heating tape and fiberglass insulation. This system allows the flow to be preheated to a set temperature, with the heating tape rated for a maximum exposure of 232 ºC. A secondary pressurized cylinder is used to store and deliver pellets which are 1mm diameter reflective glass beads. This cylinder is maintained at a constant 5 psi via a secondary line to drive the pellets through the injection line and into a 1.02 mm (0.04") injection hole located downstream of the nozzle throat. To facilitate the collection of injected pellets, a transparent container filled with water is positioned directly beneath the vertical chamber. This water serves as a medium to decelerate the pellets allowing for pellet velocity measurements via high-speed imaging from a Photron camera.

To enable rapid prototyping and the incorporation of an injection channel the converging-diverging (C-D) nozzle was fabricated using 3D printing with ABS filament. As illustrated in Fig. 5, the nozzle features a throat diameter of 5.08 mm (0.2") and an exit diameter of 7.036 mm (0.277"), yielding an area ratio (A_e/A^*) of 1.92. Based on isentropic flow relations, this geometry is designed to achieve an exit Mach number (M_e) of 2.1 under target stagnation conditions (P_0 =1.01 MPa, T_0 = 900 K) to achieve an exit velocity of 925–950 m/s. This regime closely approximates the kinetic environment of a rocket plume, providing the necessary momentum to accelerate the pellets toward a target substrate to simulate lunar landing scenarios.

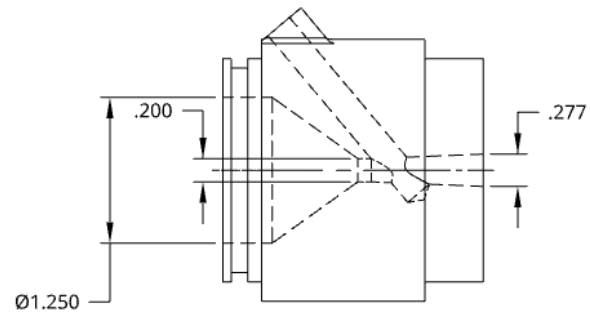

Figure 5: CAD Drawing of Nozzle Geometry

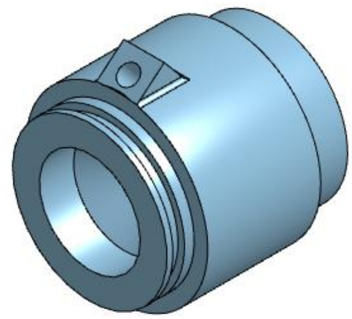

Figure 6: Isometric View of Nozzle CAD Model

B. Computational Approach

To bridge the gap between current laboratory capabilities and the project's mission requirements, a steady-state Computational Fluid Dynamics (CFD) study was conducted using ANSYS Fluent. The numerical domain utilized a 2-D axisymmetric model of the 3D-printed nozzle internal geometry.

The target stagnation conditions of P_0 =1.01 MPa and T_0 = 900 K (627 °C) were determined by using the nozzle's fixed A_e/A^* of 1.92 as the primary input in a set isentropic flow equations. While the current experimental setup is temporarily limited by the 232 °C threshold of the silicone heating tape and local atmospheric exit pressures, the CFD serves to validate the nozzle's performance at the ideal design point.

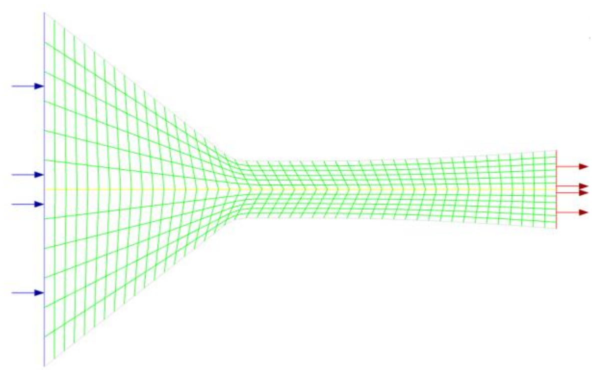

Figure 7: Mesh of Internal Nozzle Geometry

The simulation employed a pressure-based solver with an inviscid flow model, coupling the energy equation with the momentum equations to accurately resolve the exit velocity. As shown in Fig 7, the computational mesh was refined in the throat region and along the divergent section to ensure the high-speed flow field was accurately captured. These simulations provide a theoretical baseline for the exit velocity, yielding a predicted value of 925 m/s, confirming that the 3D-printed nozzle geometry can meet the design requirements once thermal constraints are addressed.

V. Diagnostics

The apparatus contains 2 thermocouples, a pressure transducer, and a high-speed camera to gather airflow data and particle velocity during the experiment. The two thermocouples used are McMaster-Carr Type K thermocouples with one placed upstream of the cylinder and one at the nozzle inlet. These are connected to a NI 9212 temperature module to collect temperature data. Upstream of the cylinder, the Ashcroft G2 pressure transducer (0-300psig) was placed in the same location as one of the thermocouples. The transducer was connected to a NI 9201 Module to gather voltage readings from the instrument. Both modules mentioned above were connected to a central NI cDAQ and LabVIEW was used for signal reading and recording.

The high-speed camera used to capture particles in the water bath was the Photron Fastcam SA3 Model 120K - M2 with a 50mm lens attachment. The lens was configured to focus on a depth that is around half the length of the 23.62”Lx16.54”Wx14.37”H water bath. This camera was controlled through the Photron FASTCAM Viewer (PFV4) software. The tests were done at 1000 and 2000 fps for test 1 and 2 respectively and a shutter speed of 1 frame per second was used for both tests. An LUT was applied to the video to clarify the images taken. The values for gain, gamma, contrast and brightness associated with the LUT are 1.00, 1.00, 0.44, 0.44 respectively. The technologies mentioned above can be seen in the Fig 8 as a schematic and in Fig 9 and Fig 10 as pictures.

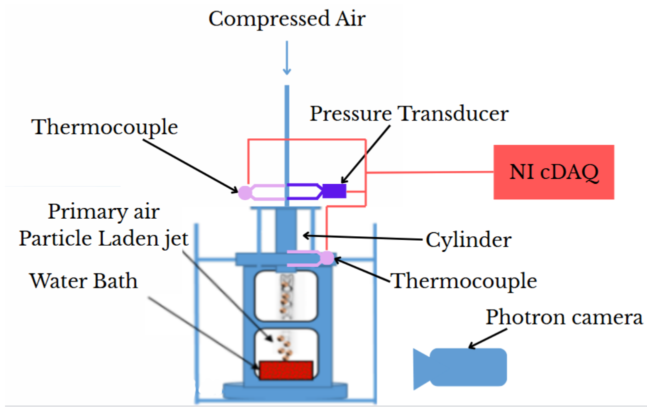

Figure 8: Schematic of diagnostics on the apparatus

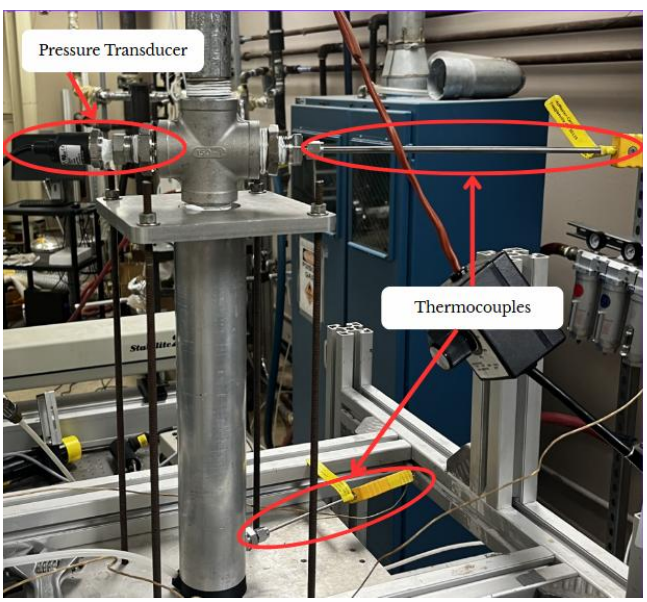

Figure 9: Picture of sensors on the apparatus

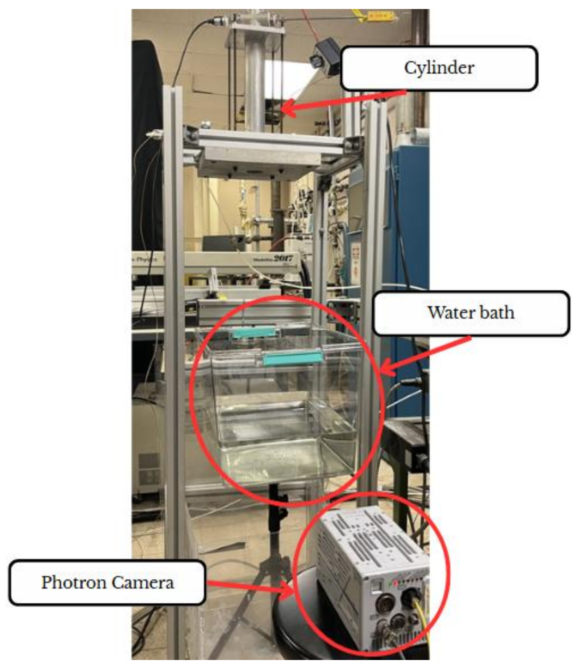

Figure 10: Picture of high-speed camera position

The LabVIEW code, shown in Figure 11, contains two DAQ assistant blocks for each of the module inputs. The pressure transducer block was configured with reading continuous samples at 500Hz sampling rate. The data was then passed through a low pass filter and a Mean PtbyPt VI to decrease noise on the reading. The temperature signal was already processed through the DAQ Assistant VI. Both signals were configured to automatically transfer to a txt file after testing to retrieve and analyze later.

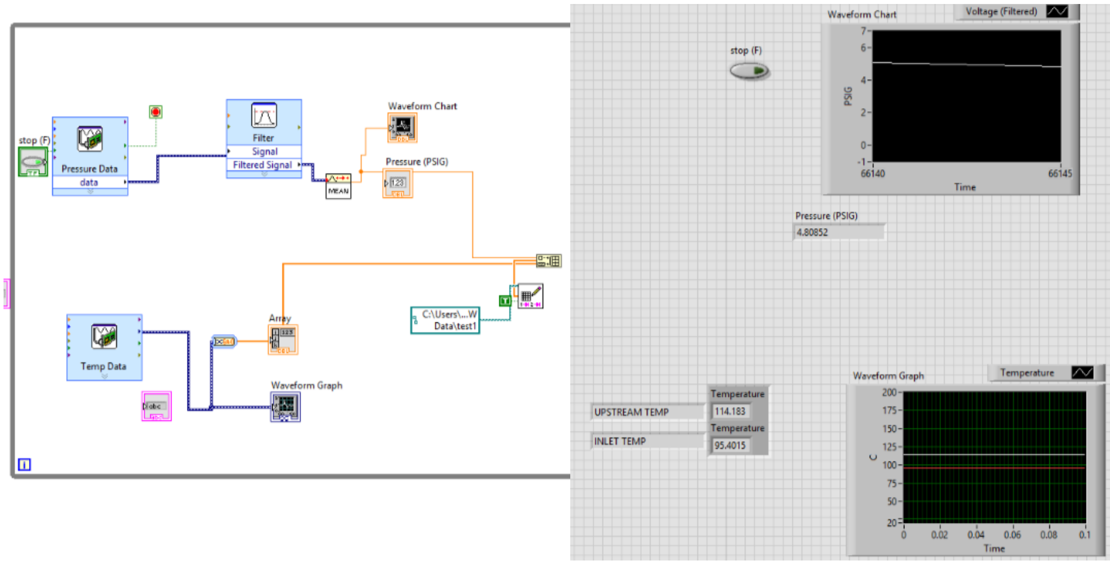

Figure 11: LabVIEW block diagram and front panel for the cDAQ

VI. Results

A. Experimental Results

Videos taken by the high-speed camera were analyzed through the built-in analysis tab in the PFV4 software. Before tests could be performed, a calibration image was taken to later relate the number of pixels to a unit length. A ruler was placed within the field of view of the camera and took a picture. The calibration image taken was then analyzed with the measurement tool. Two measurements, each for 1 mm, and one measurement for 1 cm were made. An approximation of 5 pixels per millimeter was determined as the length scale for the videos. The calibration image and measurement values in the top left can be seen in Figure 12.

Figure 12: Calibration image with measurement values

To analyze particle velocity, a range of frames were selected that clearly showed it's trajectory. Then, the distance traveled by the particle between each frame was recorded and exported to excel. The average velocity equation can then be used to calculate the average velocity of the particle at each instant of time along its trajectory. This equation is

$$v = \frac{\Delta x}{\Delta t} \tag{1}$$

where Δt is the time between each of the frames and can be defined as the inverse of the framerate. However, because particles near the surface of the water for both tests were hard to track, this method could only be used to find a velocity function of the particle traveling in water. To find the particle speed at the water's surface, the velocity function was extrapolated to show 1-3 frames before the first measured frame. To do this, first, an exponential decay function

$$v(n) = v_0 e^{-kn} \tag{2}$$

characterizing the effect of drag on velocity was used where v_0 is the initial velocity k is a constant, and n is the number of frames from t_0. With the first frame's velocity as v_0 the k was approximated by plugging in each velocity value found from the data. The average of the k values were found and plugged into Equation 2. Then, calculating for -n frames before the first recorded, an extrapolation can be made to approximate the velocity of the particle as it hits the water surface.

Two test conditions were performed. The first was run at an arbitrary pressure of 2 psi and cold flow at 23°C with the camera frame rate at 1000 fps. The resulting velocity profile is shown in Figure 13. The first and second frame shown in Figure 14 indicates the initial particle position and the approximate surface line of the water-bed. Using the extrapolation method mentioned above, the graph was extrapolated 2 frames before the first frame. The values for the velocities are shown in Table 1.

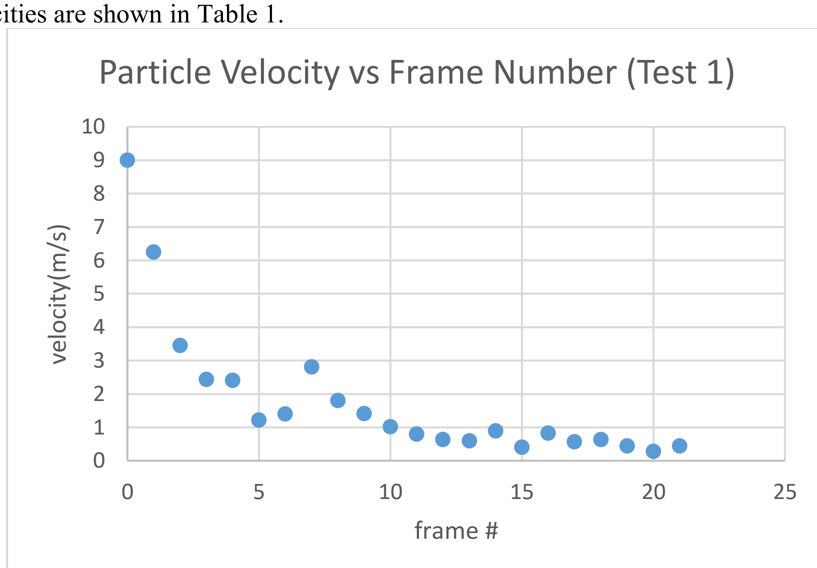

Figure 13: Velocity profile of particle for test 1

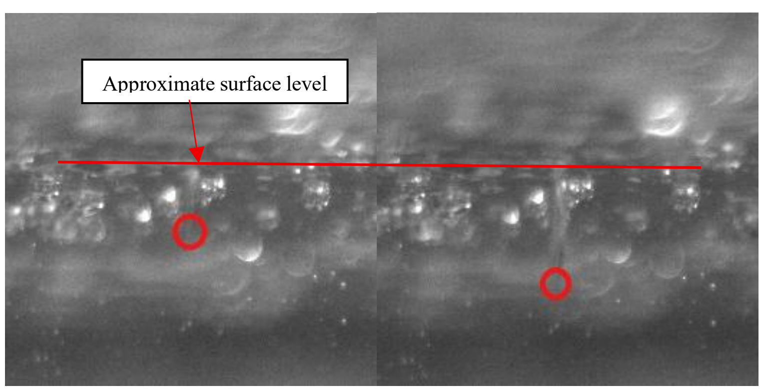

Figure 14: Frame 0(left) and 1(right) showing the travel distance in one frame near the surface

Table 1: Approximate velocity values of particle at surface (Test 1)

frame#	Velocity(m/s)
-2	14.95317
-1	11.6008

The second test condition was at a pressure of 5 psi, ~100°C at the nozzle inlet, ~120°C upstream of the cylinder and recorded at 2000 fps. This test condition yielded two particles that could be analyzed. The two particles can be seen in Fig 16. The velocity profile can associated with the particles and the approximate velocities of each particle at the water bed surface can be seen in Fig 15 and Table 2 respectively.

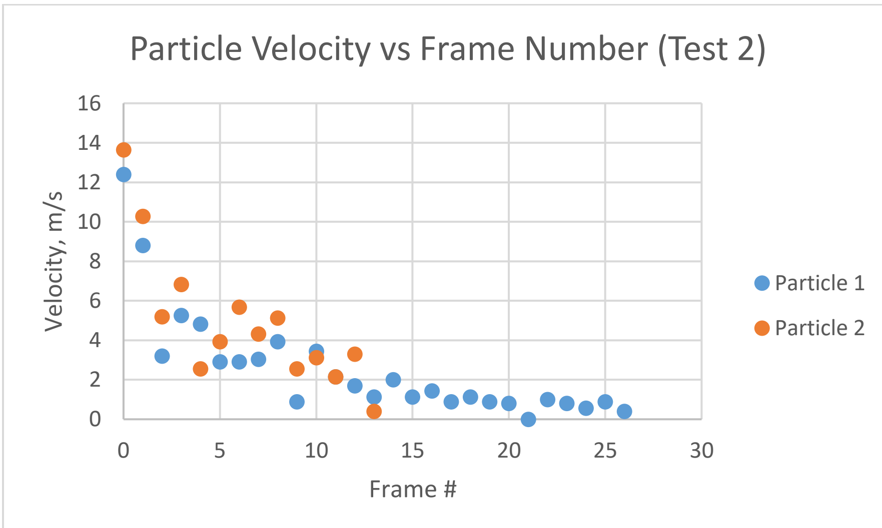

Figure 15: Velocity profile of particle for test 2

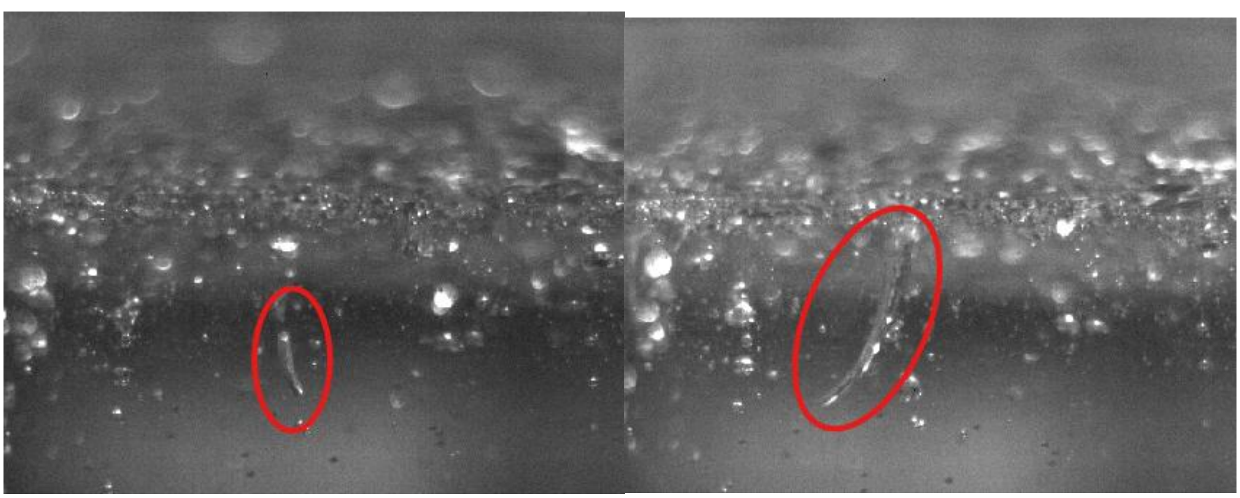

Figure 16: Image of particle 1(left) and particle 2(right)

Table 2: Approximate velocity values of particle at surface (Test 2)

Frame #	Velocity(m/s) Particle 1	Velocity(m/s) Particle 2
-2	18.93062549	20.10110336
-1	15.32520478	16.56614232

Results prove the viability of particle injection downstream of the nozzle throat to accelerate particles within the exhaust plume. With the scalability of the experiment in mind regarding temperature and pressure values, a viable proof of concept for in-situ particle embedding can be concluded.

B. Computational Results

Based on the boundary conditions utilized for the CFD simulation, an exit velocity of 925 m/s, corresponding to an exit Mach number M_e of 2.14 was observed. These 2-D CFD results serve to validate the initial calculations performed by a 1-D isentropic flow MATLAB program. This code utilizes ideal gas relations to determine the stagnation conditions required to achieve the target exit velocity for the specific nozzle geometry. The alignment between the 1-D analytical model and the 2-D numerical results provides a robust cross-check, confirming the pressure and temperature requirements for the experimental test matrix. The simulation ran in Fluent utilized inlet boundary conditions of 900 K and 1 MPa and ambient outlet conditions of 300 K and 101 kPa. Figs 17, 18, and 19 illustrate the contours of Mach number, static pressure and temperature respectively along the distance of the nozzle. This data establishes a theoretical baseline and provides a predictive framework for flow behavior once the current constraints on stagnation temperature are overcome.

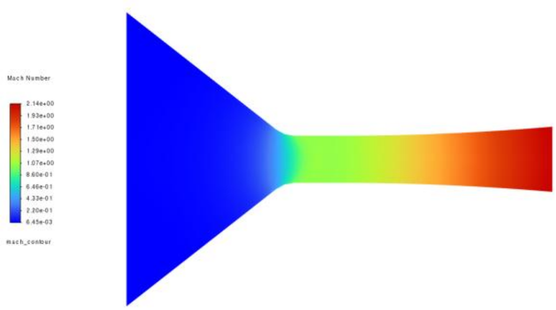

Figure 17: Mach Contour

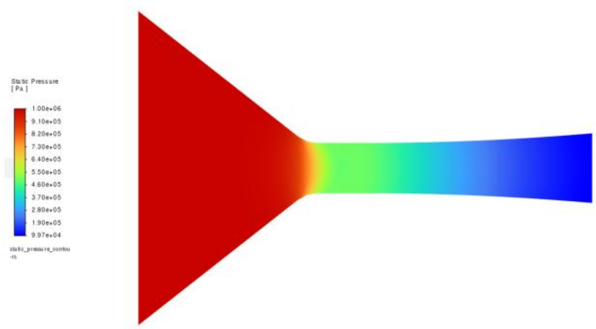

Figure 18: Static Pressure Contour

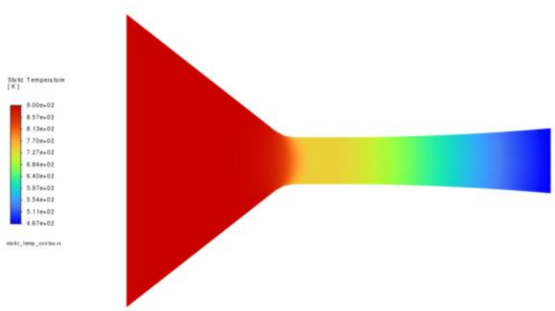

Figure 19: Static Temperature Contour

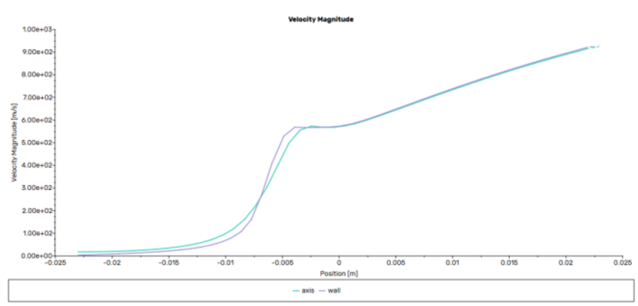

Figure 20: Velocity Along Nozzle Length

Figure 20 displays the velocity magnitude along the nozzle length. The highest rate of flow acceleration occurs near the throat region due to the "choking" effect of transitioning from the subsonic to the sonic flow regime. Beyond the throat, the flow continues to accelerate at a nearly constant rate toward supersonic speeds within the diverging section.

By strategically injecting the pellets downstream of the throat near the region where the acceleration is highest rather than at the nozzle exit, the residence time of the particles within the high-velocity stream is maximized. This increased duration within the diverging section of the nozzle allows the pellets to reach a higher exit velocity through sustained momentum transfer from the flow.

VII. Future Work

A primary goal on the computational side of the experiment is the implementation of a discrete-phase model (DPM) within the ANSYS Fluent simulation. Whereas the current inviscid model provides a benchmark solely for the flow behavior within the current nozzle geometry, the DPM will simulate how the pellets interact with the supersonic air stream. We will specifically address particle entrainment through aerodynamic drag and momentum transfer, as well as thermal coupling to predict the temperature of the pellets near the exit of the nozzle and within the plume.

To characterize the system performance, we will execute a comprehensive test matrix across a wide range of operating conditions. Future experimental cases will systematically vary the stagnation pressure and temperature to observe the conditions of the pellets within the plume. We will continue to measure the velocity of the pellets with high-speed imaging and look to incorporate particle image velocimetry (PIV) with additionally measuring temperature of the pellets using infrared (IR) imaging.

A critical component of the upcoming project phase is to collaborate with the geology research team to evaluate the mechanical properties of the cured lunar regolith samples. This interdisciplinary analysis will include an investigation of the curing, cross-linking, and binding strength of the high-temperature-resistant polymer resin with regolith under sustained heating from the exhaust plume. Final evaluations will involve compression and shear tests to confirm the ability of these plume-embedded foundations to support the weight of extraterrestrial landing and launch hardware.

VIII. Conclusion

This study presents an initial experimental and computational investigation into plume-assisted in-situ construction as a potential solution for mitigating plume–surface interaction and enabling the formation of load-bearing landing and launch pads for extraterrestrial exploration. A bench-scale cold-flow apparatus was successfully developed to demonstrate the feasibility of injecting millimeter-scale solid pellets into a supersonic flow and accelerating them toward a target medium. High-speed imaging confirmed consistent pellet entrainment and provided preliminary measurements of particle velocity, validating the core mechanics required for plume-assisted embedding.

Complementary computational fluid dynamics simulations established a theoretical baseline for the internal nozzle flow field and exit conditions. The close agreement between one-dimensional isentropic analysis and two-dimensional CFD results confirms that the selected nozzle geometry can achieve lunar-relevant exit velocities once stagnation temperature constraints are addressed. The simulations further indicate that injecting particles downstream of the throat maximizes residence time within the accelerating flow, enhancing momentum transfer and particle exit velocity.

Although current experimental limitations restrict operation at the full flow conditions representative of a rocket plume, the combined experimental and numerical results demonstrate the viability of the proposed approach as a scalable proof of concept. The ability to reliably inject and accelerate solid particles within a high-speed plume represents a critical first step toward the formation of bonded regolith composites using in-situ resources. As system is extended to higher temperatures and pressures and two phase-flow computational analysis, this work will lay the foundation for evaluating embedding behavior, and ultimately the structural performance of plume-formed surfaces.

Acknowledgments

This work is supported by NASA EPSCoR. F.A. Authors thanks Dr. Shyam Menon for continued guidance and support throughout the project. AI was used for this manuscript to assist in the writing process for the Procedure, Future Work and Conclusion sections of the paper

References

[1] N. S. Rodrigues, O. K. Tyrrell, and P. M. Danehy, "Fluorescence imaging of plume-surface interaction in large-scale reduced pressure environments," Phys. Fluids **36**, 106146 (2024). https://doi.org/10.1063/5.0223210

[2] M. Kuhns, P. Metzger, Z. Hasnain, and K. Zacny, "Instant Landing Pads for Lunar Missions," Preprint, Jan. 2018. https://www.researchgate.net/publication/377767818

[3] H. Jones and S. Menon, "Liquid jet penetration and breakup in a free supersonic gas jet," Exp. Fluids **60**, 161 (2019). https://doi.org/10.1007/s00348-019-2812-4

[4] H. Jones, "Liquid Jet Penetration and Breakup in a Free Supersonic Gas Jet," M.S. thesis, Dept. Mech. Ind. Eng., Louisiana State Univ., Baton Rouge, LA, 2018. https://repository.lsu.edu/gradschool_theses/4817

[5] M. Mehta, A. Sengupta, N. O. Renno, J. W. Van Norman, P. G. Huseman, D. S. Gulick, and M. Pokora, "Thruster Plume Surface Interactions: Applications for Spacecraft Landings on Planetary Bodies," *AIAA J.* **51** (12), 2800–2818 (2013). https://doi.org/10.2514/1.J052408

[6] P. T. Metzger, J. Vizcaino, J. A. Inman, and C. D. Immer, "Simulating the plume-surface interaction of a lunar lander," *Icarus* **210** (1), 510–513 (2010). https://doi.org/10.1016/j.icarus.2010.06.012